  Bull. Chem. Soc. Jpn., 56, 1327—1336 (1983)

Polarized Raman and Infrared Spectra of Tetramethyl- and 2,6-Dimethylpyrazines

Yoshimi Ishibashi, Fumiko Arakawa, Hiroko Shimada,* and Ryoichi Shimada†

Department of Chemistry, Faculty of Science, Fukuoka University, Nanakuma, Jonan-ku, Fukuoka 814

† *Department of Chemistry, Faculty of Science, Kyushu University 33, Hakozaki, Higashi-ku, Fukuoka 812*

(Received September 27, 1982)

The polarized Raman and infrared spectra of tetramethyl- and 2,6-dimethylpyrazines were studied. Relative intensities of the non-totally symmetric Raman bands for the tetramethylpyrazine crystal were calculated assuming the oriented gas model. Assignments of the fundamental vibrations for tetramethyl- and 2,6-dimethylpyrazines were made through the expected and observed polarization behaviors of the Raman and infrared bands and also through the normal coordinate calculation.

Although the Raman and infrared spectra of pyrazine were studied by many workers,[1-7] only a few investigations were made on the vibrational spectra of methyl-substituted pyrazines. Oertel and Myhre[8] and Bus *et al.*[9] discussed qualitative frequency shifts of the Raman and infrared bands caused by methyl substitution. Watanabe *et al.*[10] studied very recently the normal vibrations of 2-methylpyrazine based on the polarization behaviors of the Raman and infrared bands and on the normal coordinate calculation. Niimori *et al.*,[11] Lim *et al.*,[12] and Hirota *et al.*[13] investigated the natures of the lowest triplet states of tetramethyl- and 2,6-dimethylpyrazines through the kinetic and vibrational analyses of the phosphorescence emissions. They made tentative assignments of the normal vibrations without studies of the vibrational spectra.

In this work, the Raman and infrared spectra of tetramethyl- and 2,6-dimethylpyrazines were investigated and assignments of the normal vibrations were made.

Experimental

Material. The samples, tetramethyl- and 2,6-dimethylpyrazines, obtained from Aldrich Chemical Co. were purified by zone-refining of about 100 passages followed by sublimation under reduced pressure.

Optical Measurement. The polarization behavior of the Raman spectrum was observed in molten and single crystal phases with a JEOL 400 T Laser Raman Spectrophotometer. The sample was excited with the 514.5 nm line from an Ar^+ ion laser. A well-grown single crystal of tetramethylpyrazine obtained by the Bridgman method was cut along the cleavage ab plane, and the a and b crystal axes were determined by observation of the birefringence. Then the crystal was cut along the ac and bc planes and a cubic sample of about $(7\text{ mm})^3$ was obtained. As tetramethylpyrazine sublimates very quickly, Canada balsam was spread over the whole surface of the crystal sample. The method of measurement of the polarized Raman spectrum was exactly the same as that described previously.[14] Since the crystal structure of 2,6-dimethylpyrazine has not been studied yet and the crystal melts by irradiation of the laser beam at room temperature, the polarized Raman spectrum was measured in the following way. The signle crystal grown in a glass tube of about 3 mm in diameter by the Bridgman method was held in a capillary cell system of JEOL Model RS-VTC 41 in such a way that the direction of the crystal growth orients parallel to the polarization direction of the excitation laser beam. The temperature of the cell was kept at 0 °C. The Raman scattering was observed at right angles with the excitation light beam. The Raman spectrum polarized parallel to the crystal growth direction is referred to as // spectrum and the spectrum polarized perpendicular to as $\perp$ spectrum. The polarized Raman spectrum was measured for two crystal orientations. In the first orientation a sharp band at 1534 cm^{-1}, which is strong and depolarized in molten phase, appears strongly in the // spectrum and in the second orientation the 1534 cm^{-1} band appears strongly in the $\perp$ spectrum.

The infrared spectrum was observed in single crystal, liquid, vapor, and CCl_4 or CS_2 solution with a Hitachi Infrared Spectrophotometer Model 345 over the range of 4000 to 200 cm^{-1}. The single crystal was prepared in the following way. The sample was melted on a KRS-5 plate and covered with another hot KRS-5 plate. Then the two plates were put on a heated brass block and allowed to cool gradually. The crystal formed between two plates was held between two sheets of polaroid films whose polarization directions were set at right angles to each other and a single crystal portion was selected. The rest portion of the crystal was masked with a sheet of black paper. The polarized infrared spectrum was measured with the incident lights polarized parallel and perpendicular to the crystal growth direction. The first spectrum is referred to as // and the second to as $\perp$ spectrum.

Normal Coordinate Calculation

A normal coordinate calculation was performed through the standard ***GF*** matrix method with a FACOM M-200 computer at the Computer Center of Kyushu University. The structural parameter of the tetramethylpyrazine molecule was taken from the data given by Braam *et al.*[15] Since the molecular structure of 2,6-dimethylpyrazine has not been studied yet, the structural parameters of the pyrazine ring and methyl group were assumed to be the same as the data given by Wheatley[16] and by Keidel and Bauer,[17] respectively.

The ***F*** matrix elements for the in-plane vibrations were evaluated with the potential field of an improved modification of the Urey-Bradley force field.[14,18] The potential field is given by

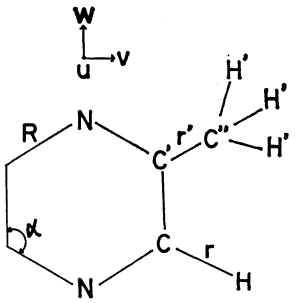

Fig. 1. Symbols for the atoms and internal coordinates.

$$V = V_{UB} + \rho[\overset{6}{\Sigma}(\Delta R,\ \Delta R)_o - \overset{6}{\Sigma}(\Delta R,\ \Delta R)_m + \overset{3}{\Sigma}(\Delta R,\ \Delta R)_p] + \Sigma k^o(\Delta r,\ \Delta r) + \Sigma k^m(\Delta r,\ \Delta r) + \Sigma h^m(\Delta R,\ \Delta\alpha) + \Sigma f^o(\Delta\alpha,\ \Delta\alpha),$$

where the symbols such as V_{UB} are the same as those used in the previous paper.[14,18] The symbols given for atoms and internal coordinates are shown in Fig. 1. For the out-of-plane vibrations the valence force field and ϕ type torsional coordinates were used. The notations of the force constants Q, q, P, p, and t are the same as those given by Whiffen.[19] In the case of the out-of-plane vibration, R and r' refer to the torsional coordinates constructing the ring and side bond, respectively. Procedure of the calculation was exactly the same as described in the previous paper.[14,18]

Calculation of Derived Polarizability Tensors

Tetramethylpyrazine crystallizes in the orthorhombic space group D_{2h}^{15} with four molecules in the unit cell, each molecule being located at the site of symmetry C_i.[15,20] The projection of the crystal structure on the ab plane is shown in Fig. 2. No factor group splitting was observed for the bands due to molecular vibrations and thus, the relationship between the derived polarizability tensors for the free molecule and crystal was derived on the basis of the simple oriented gas model. Evaluation of the matrix elements of the derived polarizability tensors of tetramethylpyrazine was made following the procedure applied for the naphthalene and anthracene crystals by Ito *et al.*[21] The derived polarizability tensor of a free molecule i with respect to the crystal-fixed coordinates is given by

$$\alpha'_{m_i}(Q_\lambda) = \boldsymbol{T}_i\, \alpha'_m(Q_\lambda)\, \tilde{\boldsymbol{T}}_i, \qquad i = 1,2,3,4,$$

where $\alpha'_m(Q_\lambda)$ is the derived polarizability tensor of a free molecule with respect to a normal vibration Q_λ, and $\boldsymbol{T}$ the transformation matrix between the molecule-fixed u, v, w and crystal-fixed a, b, c coordinates. Using the assumption of the oriented gas model and symmetry coordinates S_{Ag}, S_{B1g}, S_{B2g}, and S_{B3g} appropriate to the four molecule unit cell, the derived polarizability tensors with respect to the unit

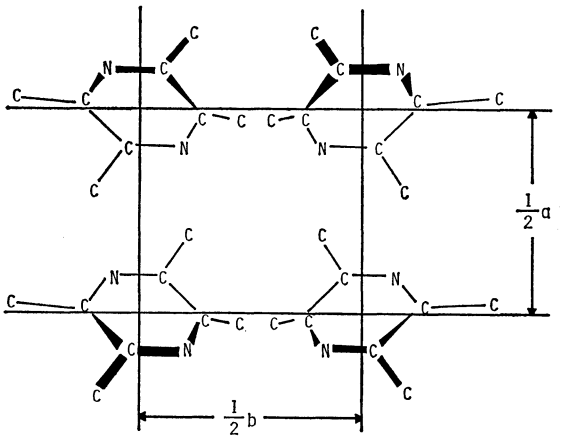

Fig. 2. Projection of the tetramethylpyrazine crystal on the ab plane.

cell vibrations are given for each symmetry species by

$$\alpha'_u(S_{Ag}) = \begin{vmatrix} A_{aa} & 0 & 0 \\ 0 & A_{bb} & 0 \\ 0 & 0 & A_{cc} \end{vmatrix},$$

$$\alpha'_u(S_{B1g}) = \begin{vmatrix} 0 & A_{ab} & 0 \\ A_{ba} & 0 & 0 \\ 0 & 0 & 0 \end{vmatrix},$$

$$\alpha'_u(S_{B2g}) = \begin{vmatrix} 0 & 0 & A_{ac} \\ 0 & 0 & 0 \\ A_{ca} & 0 & 0 \end{vmatrix},$$

$$\alpha'_u(S_{B3g}) = \begin{vmatrix} 0 & 0 & 0 \\ 0 & 0 & A_{bc} \\ 0 & A_{cb} & 0 \end{vmatrix},$$

where A's are functions of the direction cosines and the elements of the derived polarizability tensors of a free molecule.

According to the character table and selection rules for the D_{2h} molecule, we derived simple analytical expressions of A's for the vibrations belonging to different species of the molecule. These results are given in Table 1.

Results and Discussion

The force constants finally obtained after several iterative calculations for the in-plane and out-of-plane vibrations of tetramethyl- and 2,6-dimethylpyrazines are given in Table 2. The calculated vibrational frequencies and modes are given in Table 3, together with the experimental results. The molecular structures of tetramethyl- and 2,6-dimethylpyrazines were assumed to belong to the point groups D_{2h} and C_{2v}, respectively. The u axis is taken perpendicular to the molecular plane and the v and w axes in the plane with the w axis passing through the nitrogen atoms. The moments of inertia calculated from the molecular structures and the expected rotational envelopes for the infrared bands in vapor phase are given in Table 4. The depolarization measurements of the Raman spectra observed in molten phase and polarized Raman

Table 1. Elements of the derived polarizability tensors of tetramethylpyrazine

	b_{1g}	b_{2g}	b_{3g}
A_{aa}	$2a_u^{\dagger}a_v\alpha'_{uv}$	$2a_ua_w\alpha'_{uw}$	$2a_va_w\alpha'_{vw}$
A_{bb}	$2b_ub_v\alpha'_{uv}$	$2b_ub_w\alpha'_{uw}$	$2b_vb_w\alpha'_{vw}$
A_{cc}	$2c_uc_v\alpha'_{uv}$	$2c_uc_w\alpha'_{uw}$	$2c_vc_w\alpha'_{vw}$
A_{ab}	$(a_ub_v+a_vb_u)\alpha'_{uv}$	$(a_ub_w+a_wb_u)\alpha'_{uw}$	$(a_vb_w+a_wb_v)\alpha'_{vw}$
A_{ac}	$(a_uc_v+a_vc_u)\alpha'_{uv}$	$(a_uc_w+a_wc_u)\alpha'_{uw}$	$(a_vc_w+a_wc_v)\alpha'_{vw}$
A_{bc}	$(b_uc_v+b_vc_u)\alpha'_{uv}$	$(b_uc_w+b_wc_u)\alpha'_{uw}$	$(b_vc_w+b_wc_v)\alpha'_{vw}$
	a_g		
A_{aa}	$a_u^2\alpha'_{uu}+a_v^2\alpha'_{vv}+a_w^2\alpha'_{ww}$		
A_{bb}	$b_u^2\alpha'_{uu}+b_v^2\alpha'_{vv}+b_w^2\alpha'_{ww}$		
A_{cc}	$c_u^2\alpha'_{uu}+c_v^2\alpha'_{vv}+c_w^2\alpha'_{ww}$		
A_{ab}	$a_ub_u\alpha'_{uu}+a_vb_v\alpha'_{vv}+a_wb_w\alpha'_{ww}$		
A_{ac}	$a_uc_u\alpha'_{uu}+a_vc_v\alpha'_{vv}+a_wc_w\alpha'_{ww}$		
A_{bc}	$b_uc_u\alpha'_{uu}+b_vc_v\alpha'_{vv}+b_wc_w\alpha'_{ww}$		

† a_u, a_v,$\cdots c_w$ are the direction cosines of the a and u, a and v,$\cdots$c and w axes, respectively.

Table 2. Force constants for the in-plane and out-of-plane vibrations of tetramethyl- and 2,6-dimethylpyrazines

K_{N-C}	5.6 J/dm^2	H_{N-C-H}	0.24 J/dm^2	ρ	0.24 J/dm^2	P_H	0.31 aJ/rad^2
$K_{N-C'}$	5.4	$H_{C'-C''-H'}$	0.29	$k^o_{r',r'}$	0.20	$q^o_{R,R}$	−0.01
$K_{C-C'}$	5.0	$H_{H'-C''-H'}$	0.53	$k^o_{r',r}$	0.07	$q^o_{r',r'}$	0.03
$K_{C'-C''}$	3.0	$F_{C'\cdots C'}$	0.90	$k^m_{r',r'}$	0.20	$q^m_{R,R}$	−0.01
K_{C-H}	4.5	$F_{N\cdots C}$	0.55	$k^m_{r',r}$	0.06	$p^o_{C'',C''}$	0.05
$K_{C''-H'}$	4.74	$F_{C'\cdots N}$	0.70	$h^m_{R,\alpha}$	−0.12 pJ/dm rad	$p^o_{C'',H}$	0.055
$H_{C'-N-C'}$	0.30	$F_{C\cdots C}$	0.90	$f^o_{\alpha,\alpha}$	0.10 aJ/rad^2	$p^m_{C'',C''}$	−0.05
$H_{N-C'-C}$	0.55	$F_{N\cdots C''}$	0.90	$Q_{N-C'}$	0.16	$p^m_{H,H}$	−0.055
H_{C-N-C}	0.30	$F_{C\cdots C''}$	0.48	$Q_{C'-C'}$	0.22	$t^o_{R,C''}$	−0.04
$H_{N-C-C'}$	0.45	$F_{C'\cdots H}$	0.50	$Q_{C-C'}$	0.22	$t^m_{R,C''}$	−0.05
$H_{N-C'-C''}$	0.25	$F_{N\cdots H}$	0.41	Q_{N-C}	0.20	$t^o_{R,H}$	−0.02
$H_{C-C'-C''}$	0.22	$F_{C'\cdots H'}$	0.20	$Q_{C'-C''}$	0.11	$t^m_{R,H}$	−0.02
$H_{C'-C-H}$	0.25	$F_{H'\cdots H'}$	−0.20	$P_{C''}$	0.28		

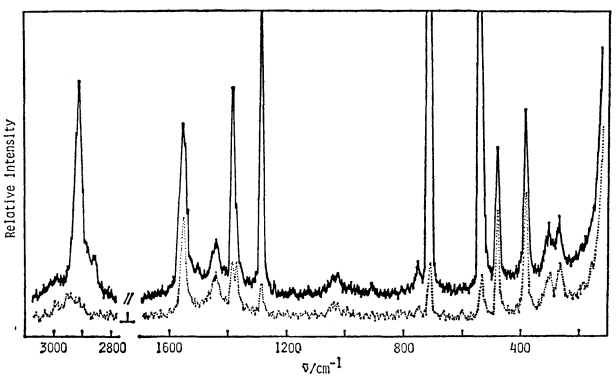

Fig. 3. Depolarization measurement of the Raman spectrum of tetramethylpyrazine.

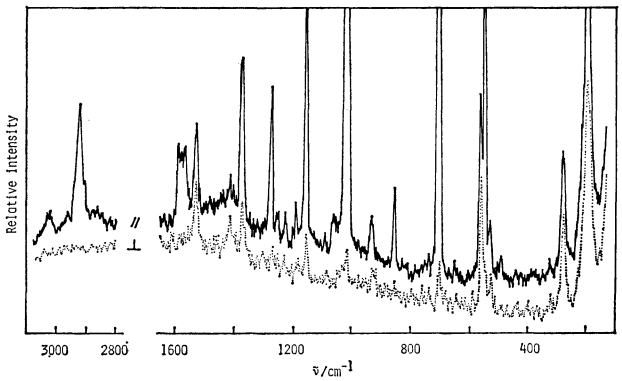

Fig. 4. Depolarization measurement of the Raman spectrum of 2,6-dimethylpyrazine.

spectra observed in single crystals of tetramethyl- and 2,6-dimethylpyrazines are shown in Figs. 3, 4, 5, and 6, respectively. The polarized Raman spectrum of tetramethylpyrazine was denoted with two symbols such as ab as used in the previous paper.[14] The first letter refers to the direction of polarization of the excitation light and the second to that of the scattering light.

The polarized Raman spectra of 2,6-dimethylpyrazine observed for the two different orientations of the crystal described in the experimental section are shown in Figs. 6 (A) and (B). We denote type α for the band whose intensity is stronger in the // spectrum than in the $\perp$ spectrum and type β for the band whose intensity is *vice versa*. The polarization behavior of a Raman band is represented by two symbols such as $\alpha\beta$, where the first and second letters refer to the polarization behaviors observed in the first and second crystal orientations and shown in Figs. 6 (A) and (B), respectively. For example, the polarization behavior

Table 3. Normal vibrations of 2,6-dimethyl- and tetramethylpyrazines

Symmetry species		Mode	2,6-Dimethylpyrazine		Tetramethylpyrazine	
C_{2v}	D_{2h}		Obsd $\tilde{\nu}$/cm^{-1}	Calcd $\tilde{\nu}$/cm^{-1}	Obsd $\tilde{\nu}$/cm^{-1}	Calcd $\tilde{\nu}$/cm^{-1}
a_1	a_g	ν_{8a} Ring	1587	1583	1547	1543
		ν_2 ϕ-CH_3 str.	1197	1210	1283	1277
		ν_1 Ring	709	706	715	734
		ν_{6a} Ring	556	548	530	531
		ν_{9a} CH_3 bend.[a]	1159	1147	296	279
	b_{1u}	ν_{19a} Ring	1450	1460	1440	1439
		ν_{12} Ring	1020	1028	1220	1207
		ν_{13} ϕ-CH_3 str.[a]	3030	3034	680	666
		ν_{18a} CH_3 bend.	420	425	310	328
b_2	b_{3g}	ν_{8b} Ring	1534	1540	1510	1522
		ν_{7b} ϕ-CH_3 str.[a]	2975	2983	1050	1069
		ν_3 CH_3 bend.[a]	1254	1240	600	580
		ν_{6b} Ring	568	559	478	465
	b_{2u}	ν_{19b} Ring	1417	1415	1410	1404
		ν_{14} Ring	1305	1304	1330	1322
		ν_{20b} ϕ-CH_3 str.	935	940	810	830
		ν_{15} CH_3 bend.	285	289	270	282
b_1	b_{2g}	ν_4 Ring	675	673	750	749
		ν_5 CH_3 wag.[a]	747	752	275	263
		ϕ-CH_3 tor.				91
	b_{3u}	ν_{16b} Ring	445	453	457	471
		ν_{11} CH_3 wag.	198	196		191
		ϕ-CH_3 tor.		160		130
a_2	b_{1g}	ν_{10a} CH_3 wag.	220	224	380	381
		ϕ-CH_3 tor.	190	171		214
	a_u	ν_{16a} Ring	415	410	550	545
		ν_{17a} CH_3 wag.[a]	955	940		268
		ϕ-CH_3 tor.				79
		Characteristic vibrations of CH_3 group				
a_1	a_g	Antisym. C–H str.			2990	2968
		Antisym. C–H str.			2930	2940
		Sym. C–H str.	2926	2921	2725	2725
		CH_3 degen. def.			1440	1441
		CH_3 sym. def.	1378	1379	1383	1375
		CH_3 rock.	856	847	920	938
	b_{1u}	Antisym. C–H str.			2985	2968
		CH_3 sym. def.			1360	1363
b_2	b_{3g}	CH_3 degen. def.			1430	1442
		CH_3 sym. def.			1367	1357
	b_{2u}	Antisym. C–H str.	2860	2863	2950	2968
		Antisym. C–H str.			2925	2940
		Sym. C–H str.	2915	2921		
		CH_3 degen. def.	1486	1486	1460	1452
		CH_3 sym. def.	1350	1362	1378	1364
		CH_3 rock.			990	970
b_1		CH_3 degen. def.	1480	1484		
		CH_3 rock.	880	884		
	b_{1g}	CH_3 degen. def.			1450	1443

a) CH_3 is replaced by H in the case of 2,6-dimethylpyrazine.

TABLE 4. POLARIZATION BEHAVIORS OF THE RAMAN AND INFRARED BANDS OF TETRAMETHYL- AND 2,6-DIMETHYLPYRAZINES

		Tetramethylpyrazine								2,6-Dimethylpyrazine			
Moment of inertia 10^{-45} kg m^2						I_w 7.61	I_v 3.80	I_u 11.2	I_w 4.32		I_u 6.49	I_v 2.27
Symmetry species of vibration		a_g	b_{1g}	b_{2g}	b_{3g}	a_u	b_{1u}	b_{2u}	b_{3u}	a_1	a_2	b_1	b_2
Infrared	Vapor (Rotational band type)						B	A	C	B		C	A
	Crystal						I[a]	II[a]	III[a]	II[a]		III[a]	I[a]
Raman	Liquid	p	dp	dp	dp					p	dp	dp	dp
	Crystal		cc ab	aa cc	bb cc					$\alpha\alpha$[a]	$\beta\beta$[a]	$\alpha\beta$[a]	

a) These polarization behaviors were experimentally determined by comparison with the band envelope in the infrared vapor spectrum.

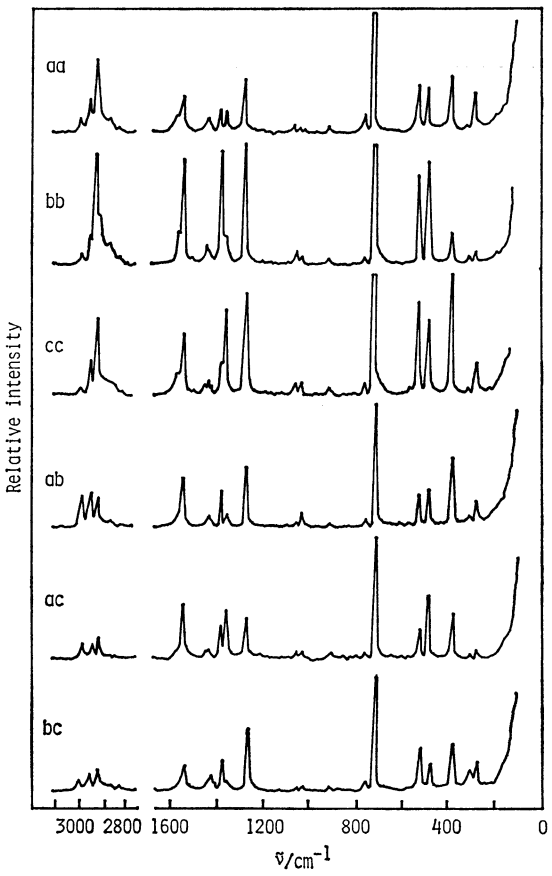

Fig. 5. Polarized Raman spectrum of the tetramethylpyrazine single crystal.

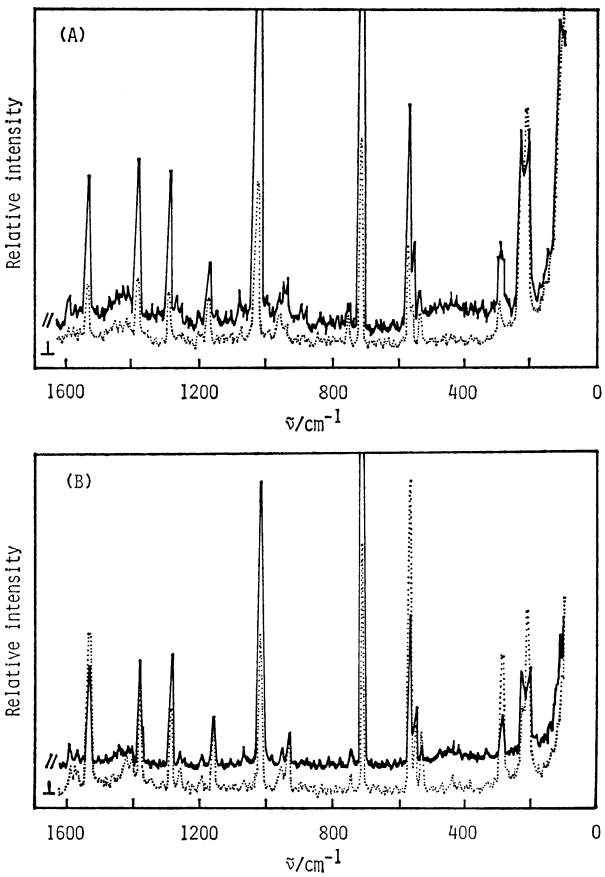

Fig. 6. Polarized Raman spectrum of the 2,6-dimethylpyrazine single crystal. For the polarization behaviors of the (A) and (B), see text.

of the 1534 cm^{-1} band is represented by $\alpha\beta$. The observed polarization behaviors of the non-totally symmetric Raman bands can be classified into three types $\alpha\alpha$, $\beta\beta$, and $\alpha\beta$ through which each Raman band can be experimentally assigned to a certain symmetry species.

The polarized infrared spectra of tetramethyl- and 2,6-dimethylpyrazines are shown in Figs. 7 and 8, respectively. The infrared crystal bands can be classified into three types I, II, and III based on their polarization behaviors. In the first type, the intensities of the // and ⊥ components of the bands are nearly equal to each other. In the second type, the intensity of the // component is stronger than that of the ⊥ one, and in the third type, the intensity of the ⊥ component is much stronger than that of the // one.

Tetramethylpyrazine. The direction cosines between the crystal and molecular axes were calculated using the X-ray diffraction data given by Braam *et al.*[15] and the matrix elements of the derived polarizability tensor listed in Table 1 were evaluated. Squares of the calculated elements of the derived polarizability tensors, which are proportional to the Raman intensities, are given in Table 5 for the non-totally g symmetric vibrations. In this calculation,

Table 5. Squared values of the elements of the derived polarizability tensors for tetramethylpyrazine

	b_{1g}	b_{2g}	b_{3g}
$(A_{aa})^2$	0.19	0.76	0.10
$(A_{bb})^2$	0.08	0.06	0.91
$(A_{cc})^2$	0.53	0.39	0.41
$(A_{ab})^2$	0.40	0.15	0.05
$(A_{ac})^2$	0.10	0.01	0.24
$(A_{bc})^2$	0.10	0.23	0.00

values of the derived polarizability tensors of the free molecule, α'_{uv}, α'_{uw}, and α'_{vw}, are taken to be 1 in order to discuss the relative intensities of the Raman bands belonging to a certain symmetry species. It is expected from Table 5 that the b_{1g} vibrations appear strongly in the cc and ab spectra, the b_{2g} vibrations in the aa and cc spectra and the b_{3g} vibrations in the bb and cc spectra. These expected polarization behaviors of the Raman bands are given in Table 4.

a_g Species: Strongly polarized Raman bands observed at 1547, 1383, 1283, 715, and 530 cm^{-1} in the depolarization measurements were directly ascribed to the a_g vibrations and assigned to the ν_{8a}, ν_{CH_3} symmetric deformation, $\nu_2(\phi\text{-}CH_3$ stretching), ν_1, and ν_{6a} vibrations, respectively based on the calculation. A very broad and almost depolarized Raman band observed around 300 cm^{-1} in liquid phase splits into two bands at 305 and 296 cm^{-1} in the single crystal Raman spectrum. The polarization behavior of the 305 cm^{-1} band corresponds to the b_{3g} vibration, while that of the 296 cm^{-1} band does not correspond to any non-totally symmetric vibrations. Therefore, the 296 cm^{-1} band was assigned to the totally symmetric $\nu_{9a}(CH_3$ bending) vibration.

b_{3g} Species: A Raman band observed at 478 cm^{-1} has strong intensity in the bb spectrum and medium intensity in the cc spectrum. Raman bands observed at 1510 and 1050 cm^{-1} have rather weak intensities in the bb and cc spectra and extremely weak intensities in all other spectra. Table 4 indicates that the polarization behaviors of these bands are consistent with the b_{3g} vibration. Therefore, the 1510, 1050, and 478 cm^{-1} bands were assigned to the ν_{8b}, ν_{7b} ($\phi\text{-}CH_3$ stretching), and ν_{6b} vibrations of b_{3g} species, respectively. A very weak Raman band at 600 cm^{-1} was observed only in the bb spectrum and thus this band was assigned to the $\nu_3(CH_3$ bending) vibration.

b_{1g} Species: A Raman band observed at 380 cm^{-1} has strong intensity in the cc spectrum and medium intensity in the ab and aa spectra. These polarization behaviors are consistent with the b_{1g} vibration. Thus the 380 cm^{-1} band was assigned to the ν_{10a} (CH_3 wagging) vibration.

b_{2g} Species: A Raman band observed at 275 cm^{-1} has stronger intensity in the aa and cc spectra compared with those in other spectra. A Raman band observed at 750 cm^{-1} decreases its intensity in the order of aa>cc>bc≈ab>bb≈ac spectra. These polarization behaviors definitely indicate that the 275 and 750 cm^{-1} bands have to be assigned to the b_{2g} vibration and hence assigned to the ν_5 (CH_3 wagging) and ν_4 vibrations, respectively.

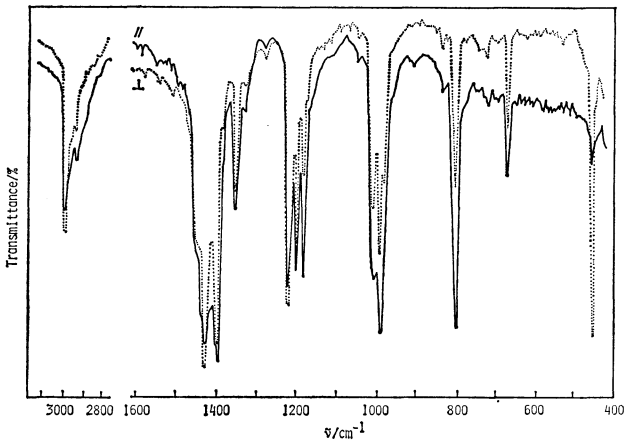

Fig. 7. Polarized infrared spectrum of the tetramethylpyrazine single crystal.

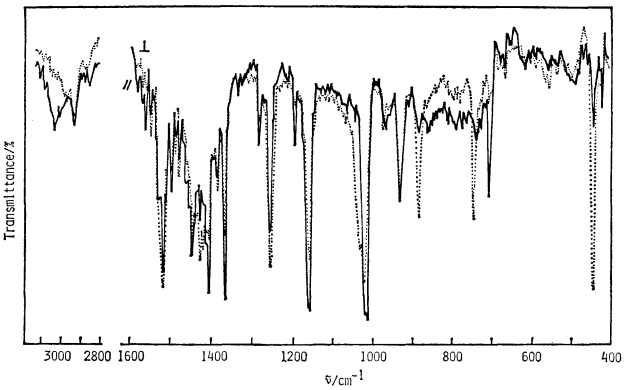

Fig. 8. Polarized infrared spectrum of the 2,6-dimethylpyrazine single crystal.

The assignment of a Raman band observed at 1367 cm^{-1} is rather difficult. This band is depolarized in the molten Raman spectrum, while its polarization behavior in the crystal Raman spectra does not correspond to any non-totally symmetric vibrations. Therefore, this band was tentatively assigned to the superposition of the CH_3 symmetric deformation vibration of b_{3g} species and the overtone vibration of the $\nu_{13}(\phi\text{-}CH_3$ stretching) vibration.

b_{1u} Species: According to Table 4, the infrared b_{1u} band is expected to show the B type band envelope in vapor. Infrared bands observed at 1360 and 1220 cm^{-1} showed the B band type in vapor and the type I polarization behavior in crystal. Since the band envelope and polarization behavior of the infrared band directly depend on the direction of the transition moment, it is expected that the infrared bands showing the type I polarization behavior in crystal should be assigned to the b_{1u} vibration. Strong infrared bands observed at 1440 and 1220 cm^{-1}, a medium intense band at 1360 cm^{-1} and a weak band at 680 cm^{-1} show the type I behavior in crystal and thus these bands were assigned to the ν_{19a}, ν_{12}, ν_{CH_3} symmetric deformation, and $\nu_{13}(\phi\text{-}CH_3$ stretching) vibrations of

TABLE 6. VIBRATIONAL ANALYSES OF THE RAMAN AND INFRARED SPECTRA OF TETRAMETHYLPYRAZINE

Raman				Infrared				
Liquid			Crystal Pol.	Solution		Crystal Pol.	Vapor type	Assignment
$\tilde{\nu}$/cm^{-1}	Int.	Pol.		$\tilde{\nu}$/cm^{-1}	Int.			
2990	m	p						antisym. C-H str. (a_g)
				2985	w	I		antisym. C-H str. (b_{1u})
				2950	m	II		antisym. C-H str. (b_{2u})
2935	sh	dp	cc,ab					$2\nu_2+\nu_{10a}$ (b_{1g})
2930	s	p						antisym. C-H str. (a_g)
				2925	m	II		antisym. C-H str. (b_{2u})
2868	vw	p						$2\nu_2+\nu_{9a}$ (a_g)
2820	vw	p						$\nu_2+\nu_{8a}$ (a_g)
2760	vw	p						$2CH_3$ sym. def. (a_g)
2725	vw	p						sym. C-H str. (a_g)
2580	vw	p						$2\nu_2$ (a_g)
1555	m	dp	aa,cc					$\nu_2+\nu_5$ (b_{2g})
1547	s	p						ν_{8a} (a_g)
1510	vw	dp	bb,cc					ν_{8b} (b_{3g})
				1460	sh	II		CH_3 degen. def. (b_{2u})
1450	m		cc,ab					CH_3 degen. def. (b_{1g})
1440	m	p						CH_3 degen. def. (a_g)
				1440	s	I		ν_{19a} (b_{1u})
1430	m		bb,cc					CH_3 degen. def. (b_{3g})
				1410	vs	II		ν_{19b} (b_{2u})
				1403	s	I		$\nu_{20b}+\nu_3$ (b_{1u})
1383	s	p						CH_3 sym. def. (a_g)
				1378	sh	II		CH_3 sym. def. (b_{2u})
1367	m	dp						CH_3 sym. def. (b_{3g}) $2\nu_{13}$ (a_g)
				1360	m	I	B	CH_3 sym. def. (b_{1u})
				1330	vw	II		ν_{14} (b_{2u})
1283	s	p						ν_2 (ϕ-CH_3 str.) (a_g)
				1280	vw	I		$\nu_{6b}+\nu_{20b}$ (b_{2u})
				1220	s	I	B	ν_{12} (b_{1u})
				1200	m	I		$\nu_{6a}+\nu_{13}$ (b_{1u})
				1180	m	II		CH_3 rock.$+\nu_{15}$ (b_{2u})
1050	w	dp	bb,cc					ν_{7b} (ϕ-CH_3 str.) (b_{3g})
1030	w	p						$\nu_4+\nu_5$ (a_g)
				1015	m	I		$\nu_1+\nu_{18a}$ (b_{1u})
				990	s	II		CH_3 rock. (b_{2u})
				970	sh	I		$\nu_{9a}+\nu_{13}$ (b_{1u})
920	vw	p						CH_3 rock. (a_g)
				835	vw	I		$\nu_{6a}+\nu_{18a}$ (b_{1u})
				810	m	II	A	ν_{20b} (ϕ-CH_3 str.) (b_{2u})
750	w	dp	aa,cc					ν_4 (b_{2g})
				730	w	I		$\nu_5+\nu_{16b}$ (b_{1u})
715	vs	p						ν_1 (a_g)
				680	w	I		ν_{13} (ϕ-CH_3 str.) (b_{1u})
600	vw	dp	bb					ν_3 (CH_3 bend.) (b_{3g})
550[a]	vw			545[a]	vw			ν_{16a} (a_u)
530	s	p						ν_{6a} (a_g)
478	s	dp	bb,cc					ν_{6b} (b_{3g})
				457	m	III	C	ν_{16b} (b_{3u})
380	s	dp	cc,ab					ν_{10a} (CH_3 wag.) (b_{1g})
				310[b]	w			ν_{18a} (CH_3 bend.) (b_{1u})
305	vw	dp	bb,cc					tor.+tor'. (b_{3g})
296	vw	p?						ν_{9a} (CH_3 bend.) (a_g)
275	m	dp	aa,cc					ν_5 (CH_3 wag.) (b_{2g})
				270[b]	vw			ν_{15} (CH_3 bend.) (b_{2u})

a) Observed in crystal phase. b) Observed in liquid phase.

Table 7. Vibrational analyses of the Raman and infrared spectra of 2,6-dimethylpyrazine

Raman				Infrared				Assignment
Liquid			Crystal Pol.	Liquid		Crystal Pol.	Vapor type	
$\tilde{\nu}$/cm^{-1}	Int.	Pol.		$\tilde{\nu}$/cm^{-1}	Int.			
3030	w	p		3030	s	II		ν_{13} (a_1)
2975	vw	dp		2965	m		A	ν_{7b} (b_2)
2926	m	p						sym. C-H str. (in CH_3) (a_1)
2915	vw			2920	m	I		sym. C-H str. (in CH_3) (b_2)
2860	vw	dp		2855	vw	I		antisym. C-H str. (in CH_3) (b_2)
1587	m	p		1584	vw	II		ν_{8a} (a_1)
1575	w	p		1563	vw	II		$\nu_{12}+\nu_{6a}$ (a_1)
				1550	w	I		$\nu_3+\nu_{18a}$ (b_2)
1534	m	dp	$\alpha\beta$	1535	s	I	A	ν_{8b} (b_2)
				1486	w	I		CH_3 degen. def. (b_2)
				1480	w	III		CH_3 degen. def. (b_1)
1450	vw	p		1452	w	II		ν_{19a} (a_1)
1417	w	dp	$\alpha\beta$	1420	m	I	A	ν_{19b} (b_2)
				1418[a]	w	III		$\nu_{6a}+CH_3$ rock. (b_1)
1405[a]				1410	m	II		$2\nu_1$ (a_1)
				1383	w	III		$\nu_{9a}+CH_3$ wag. (b_1)
1378	m	p		1367	m	II	B	CH_3 sym. def. (a_1)
1350	vw		$\alpha\beta$	1359	w	I		CH_3 sym. def. (b_2)
1305	vw	dp		1305[b]	vw			ν_{14} (b_2)
1278	m	p		1280	w	II		$\nu_1+\nu_{6a}$ (a_1)
1254	w	dp	$\alpha\beta$	1255	vs	I	A	ν_3 (b_2)
1197	w	p		1197	vw	II		ν_2 (ϕ-CH_3 str.) (a_1)
1159	m	p		1159	vs	II	B	ν_{9a} (a_1)
1070	w		$\alpha\alpha$	1060[b]	vw			$\nu_{10a}+CH_3$ rock. (a_2)
				1020	m	III		$\nu_{18a}+\nu_5$ (b_1)
1020	s	p		1016	vs	II	B	ν_{12} (a_1)
				970	w	I		$\nu_5+\nu_{10a}$ (b_2)
955	w	dp	$\alpha\alpha$					ν_{17a} (a_2)
935	w	dp	$\alpha\beta$	932	m	I	A	ν_{20b} (ϕ-CH_3 str.) (b_2)
890	w							$2\nu_{16b}$ (a_1)
880	w		$\beta\beta$	870	s	III	C	CH_3 rock. (b_1)
856	m	p						CH_3 rock. (a_1)
747	w	dp	$\beta\beta$	745	m	III		ν_5 (b_1)
709	vs	p		707	w	II		ν_1 (a_1)
675	w	dp						ν_4 (b_1)
568	m	dp	$\alpha\beta$	570[b]	w			ν_{6b} (b_2)
556	s	p						ν_{6a} (a_1)
535	w	dp	$\beta\beta$					(b_1)
500	vw	dp						$\nu_{18a}+\nu_{10a}$ (a_2)
445	vw	dp		444	vs	III	C	ν_{16b} (b_1)
420	vw			420[b]	w			ν_{18a} (CH_3 bend.) (a_1)
415	vw	dp						ν_{16a} (a_2)
325	vw	dp						
285	m	dp	$\alpha\beta$	280[b]	w			ν_{15} (CH_3 bend.) (b_2)
220	m	dp	$\alpha\alpha$	225[b]	w			ν_{10a} (CH_3 wag.) (a_2)
198	s	dp	$\beta\beta$					ν_{11} (CH_3 wag.) (b_1)
190	sh	dp	$\alpha\alpha$					ϕ-CH_3 tor. (a_2)

a) Observed in crystal phase. b) Observed in liquid phase.

b_{1u} species, respectively. A weak infrared band found at 310 cm^{-1} in liquid was tentatively assigned to the ν_{18a} (CH_3 bending) vibration based on the calculation.

b_{2u} Species: A medium intense infrared band observed at 810 cm^{-1} showed the A band type in vapor. From Table 4, this band was ascribed to the b_{2u} vibration. This band showed the type II polarization behavior in crystal. Therefore, the infrared bands at 1410, 1330, and 810 cm^{-1} showing the type II character in crystal were assigned to the ν_{19b}, ν_{14}, and ν_{20b}

(ϕ-CH_3 stretching) vibrations of b_{2u} species, respectively. A weak band observed at 270 cm^{-1} in liquid was assigned to the ν_{15} (CH_3 bending) vibration based on the calculation.

b_{3u} Species: As a medium intense bands observed at 457 cm^{-1} showed the typical C band type in vapor, this band was definitely ascribed to the b_{3u} vibration and assigned to the ν_{16b} vibration. The CH_3 wagging and ϕ-CH_3 torsional vibrations belonging to b_{3u} species were not detected in the infrared spectrum because of their low frequencies.

a_u Species: Extremely weak infrared and Raman bands observed at 545 and 550 cm^{-1}, respectively, in crystal might be assigned to the ν_{16a} vibration of a_u species. These bands are considered to appear in the spectra by the crystal force distorsion.

2,6-Dimethylpyrazine. a_1 Species: Strong and polarized Raman bands observed at 3030, 1587, 1450, 1197, 1159, 1020, 709, and 556 cm^{-1} in molten phase were straightforwardly assigned to the totally symmetric ν_{13}, ν_{8a}, ν_{19a}, ν_2(ϕ-CH_3 stretching), ν_{9a}, ν_{12}, ν_1, and ν_{6a} vibrations, respectively. The corresponding infrared bands showed the type II polarization in crystal and the B band type in vapor. A very weak Raman band at 420 cm^{-1} was assigned to the totally symmetric ν_{18a}(CH_3 bending) vibration based on the calculation.

b_1 Species: A very strong infrared band at 444 cm^{-1} showed the typical C band type in vapor and the type III polarization behavior in crystal. An infrared band at 745 cm^{-1} showed the type III behavior and a depolarized Raman band at 747 cm^{-1} showed the $\beta\beta$ polarization behavior in crystal. According to Table 4, the 444 and 745 cm^{-1} bands should be assigned to the b_1 vibrations and thus assigned to the ν_{16b} and ν_5 vibrations, respectively. A Raman band at 198 cm^{-1} showed the $\beta\beta$ character in crystal and thus this band was assigned to the ν_{11}(CH_3 wagging) vibration of b_1 species. Depolarized Raman band at 675 cm^{-1} was assigned to the ν_4 vibration based on the calculation.

b_2 Species: The infrared bands having the A band envelope in vapor showed the type I polarization behavior in crystal and the corresponding Raman band showed the $\alpha\beta$ polarization character in crystal. According to Table 4, the band showing these polarization behaviors could be assinged to the b_2 vibration. Infrared bands observed at 2965, 1535, 1420, 1255, and 932 cm^{-1} showing the A band type in vapor were assigned to the ν_{7b}, ν_{8b}, ν_{19b}, ν_3, and ν_{20b}(ϕ-CH_3 stretching) vibrations, respectively. Raman bands at 568 and 285 cm^{-1} showed the $\alpha\beta$ polarization character in crystal and assigned to the ν_{6b} and ν_{15}(CH_3 bending) vibrations, respectively. A weak and depolarized Raman band at 1305 cm^{-1} was assigned to the ν_{14} vibration based on the calculation.

a_2 Species: Depolarized Raman bands observed at 955, 220, and 190 cm^{-1} showed the $\alpha\alpha$ polarization character in crystal. These bands were assigned to the ν_{17a}, ν_{10a}(CH_3 wagging), and ϕ-CH_3 torsional vibrations of a_2 species, respectively, because the Raman bands showing the $\beta\beta$ and $\alpha\beta$ polarization behaviors in crystal were already assigned to the b_1 and b_2 vibrations, respectively. A weak and depolarized Raman band at 415 cm^{-1} was assigned to the ν_{16a} vibration based on the calculation.

The characteristic vibrations for CH_3 group of tetramethyl- and 2,6-dimethylpyrazines were determined based on the observed polarization behaviors of the Raman and infrared bands as well as the normal coordinate calculation. Detailed vibrational analyses of the Raman and infrared spectra are given in Tables 6 and 7, and the normal vibrations are summarized in Table 3.

The normal coordinate calculation made for tetramethylpyrazine suggests that the ν_1, ν_{12}, ν_{6b}, ν_{14}, and ν_{16a} vibrations in this molecule couple with the ϕ-CH_3 stretching (ν_2), ϕ-CH_3 stretching (ν_{13}), CH_3 bending (ν_3), ϕ-CH_3 stretching (ν_{20b}), and CH_3 wagging (ν_{17a}) vibrations, respectively. Observed vibrational frequencies of the ν_1 and ν_{6b} vibrations are lower and the frequencies of the ν_{12}, ν_{14}, and ν_{16a} vibrations are higher than those of the corresponding vibrations of pyrazine. These observation are consistent with the calculated results mentioned above. In 2,6-dimethylpyrazine the CH_3 group concerned with the ϕ-CH_3 stretching (ν_{13}), CH_3 bending (ν_3), and CH_3 wagging (ν_{17a}) vibrations is replaced with the H atom and these vibrations do not couple with the ν_{12}, ν_{6b}, and ν_{16a} vibrations, respectively. Therefore, the observed vibrational frequencies of ν_{12}, ν_{6b}, and ν_{16a} vibrations are nearly the same as those of pyrazine, while the frequency of the ν_1 vibration is lower and that of the ν_{14} vibration is higher than those of pyrazine.

We believe that the assignment of the normal vibrations given for tetramethyl- and 2,6-dimethylpyrazines are reliable and quite useful in the reasonable vibrational analyses of the phosphorescence spectra of these molecules.

References

1) R. C. Lord, A. J. Marson, and F. A. Miller, *Spectrochim. Acta*, **9**, 113 (1957).

2) J. D. Simmons, K. K. Innes, and G. M. Begun, *J. Mol. Spectrosc.*, **14**, 190 (1964).

3) S. Califano, G. Adembri, and G. Sbrana, *Spectrochim. Acta*, **20**, 385 (1964).

4) K. K. Innes, J. P. Byrne, and I. G. Ross, *J. Mol. Spectrosc.*, **22**, 125 (1967).

5) G. Sbrana, V. Schettino, and R. Righini, *J. Chem. Phys.*, **59**, 2441 (1973).

6) J. Zarembowitch and L. Bokobza-Sebagh, *Spectrochim. Acta, Part A*, **32**, 605 (1976).

7) I. Suzuki, Y. Udagawa, and M. Ito, *Chem. Phys. Lett.*, **64**, 333 (1979).

8) R. P. Oertel and D. V. Myhre, *Anal. Chem.*, **44**, 1589 (1972).

9) J. Bus, Th. J. Liefkens, and W. Schwaiger, *Recl. Trav. Chim. Pays-Bas*, **92**, 123 (1973).

10) T. Watanabe, H. Shimada, and R. Shimada, *Bull. Chem. Soc. Jpn.*, **55**, 2564 (1982).

11) K. Niimori, K. Fukuda, N. Nishi, and M. Kinoshita, Symposium on the Molecular Structure and Molecular Electronic Structure, Tokyo, October 1974, Abstr. No. 20A10.

12) S. L. Madej, G. D. Gillispie, and E. C. Lim, *Chem. Phys.*, **32**, 1 (1978).

13) K. Miyake, S. Yamauchi, and N. Hirota, Symposium

on the Molecular Structure and Molecular Electronic Structure, Fukuoka, October 1980, Abstr. No. 4B19.
14) Y. Ishibashi, R. Shimada, and H. Shimada, *Bull. Chem. Soc. Jpn.*, **55**, 2765 (1982).
15) A. W. M. Braam, A. Eshuis, and A. Vos, *Acta Crystallogr., Sect. B*, **37**, 730 (1981).
16) P. J. Wheatley, *Acta Crystallogr.*, **10**, 182 (1957).
17) F. A. Keidel and S. H. Bauer, *J. Chem. Phys.*, **25**, 1218 (1956).
18) S. Kizuki, Y. Ishibashi, H. Shimada, and R. Shimada, *Mem. Fac. Sci. Kyushu Univ., Ser. C*, **13**, 7 (1981).
19) D. H. Whiffen, *Philos. Trans. R. Soc. London, Ser. A*, **248**, 131 (1955).
20) D. T. Cromer, A. J. Ihde, and H. L. Ritter, *J. Am. Chem. Soc.*, **73**, 5587 (1951).
21) M. Suzuki, T. Yokoyama, and M. Ito, *Spectrochim. Acta, Part A*, **24**, 1091 (1968).